RESEARCH ARTICLE

Natural Products

Natural α-glucosidase inhibitors from selected medicinal plants in Malaysia

SY Liew[1,6], Y Sivasothy[2], NN Shaikh[3], K Javaid[3], DM Isa[4], VS Lee[4], MI Choudhary[3,5] and K Awang[4,6*]

[1] *Chemistry Division, Centre for Foundation Studies in Science, Universiti Malaya, 50603 Kuala Lumpur, Malaysia.*

[2] *School of Pharmacy, Monash University Malaysia, Jalan Lagoon Selatan, 47500 Bandar Sunway, Selangor Darul Ehsan, Malaysia.*

[3] *H. E. J. Research Institute of Chemistry, International Center for Chemical and Biological Sciences, University of Karachi, Karachi-75270, Pakistan.*

[4] *Department of Chemistry, Faculty of Science, Universiti Malaya, 50603 Kuala Lumpur, Malaysia.*

[5] *Department of Biochemistry, Faculty of Science, King Abdulaziz University, Jeddah-214412, Saudi Arabia.*

[6] *Centre for Natural Products Research and Drug Discovery (CENAR), Universiti Malaya, 50603 Kuala Lumpur, Malaysia.*

Abstract: The most prevalent subtype of diabetes is Type 2 Diabetes Mellitus which results from an abnormal postprandial increase in blood glucose. Inhibition of the carbohydrate-hydrolysing enzymes (alpha-glucosidase and alpha-amylase) in the human digestive organs can control blood glucose levels, making it an important strategy in the management of Type 2 Diabetes Mellitus. A majority of the oral synthetic drugs which have been developed to treat Type 2 Diabetes Mellitus are expensive and have undesirable side effects. As a result, plant-derived remedies have become preferred alternatives as they are easily available, affordable and less harmful. Angustine (**1**) the major constituent in *Nauclea subdita* (Korth.) Steud., and (*E*)-labda-8(17),12-dien-15,16-dial (**2**) and zerumin A (**3**) of *Alpinia pahangensis* Ridley were evaluated for their α-glucosidase inhibitory activity. (*E*)-Labda-8(17),12-dien-15,16-dial (**2**) (IC_{50} = 39.7 μM) was identified as the most potent inhibitor among all three, followed by angustine (**1**) (IC_{50} = 48.1 μM) and zerumin A (**3**) (IC_{50} = 53.3 μM). Enzyme kinetic studies indicated that angustine (**1**) was a mixed-type inhibitor, while (*E*)-labda-8(17),12-dien-15,16-dial (**2**), and zerumin A (**3**) were non-competitive inhibitors. Molecular docking and molecular dynamics (MD) simulation studies were performed to predict the key interactions between the ligands and the target protein, 1AGM (complex of acarbose with glucoamylase from *Aspergillus awamori*). The results of the study of binding interaction energy suggested that angustine (**1**) has the potential to be used as a natural drug lead in the treatment of type 2 diabetes mellitus.

Keywords: α-glucosidase, *Alpinia pahangensis*, angustine, (*E*)-labda-8(17),12-dien-15,16-dial, molecular docking, *Nauclea subdita*.

INTRODUCTION

Diabetes mellitus (D.M.) is a chronic metabolic disorder which has become a global health problem. According to the World Health Organization (WHO) Global Report on Diabetes, 422 million adults were estimated to live with diabetes in 2014, almost quadruple compared to 108 million in 1980 (WHO, 2016). This drastic rise was due to the increase in type 2 diabetes mellitus (T2DM) (WHO, 2016). Postprandial hyperglycaemia is one of the earliest signs of T2DM, which results from insufficient insulin secretion (Sun *et al.*, 2016). α-Glucosidase plays an important role in catalysing the hydrolysis of carbohydrates *i.e*., cleavage of the terminal non-reducing 1-4 linked α-D-glucose residues and the release of α-D-glucose (Simpson *et al.*, 2012). Inhibition of this enzyme is a validated strategy to treat and prevent T2DM by decreasing postprandial hyperglycaemia (Sun *et al*., 2016). The current clinical α-glucosidase inhibitors (acarbose, voglibose, and miglitol) are widely used for the treatment of T2DM (Liu *et al.*, 2016). However, they are reported to cause many adverse effects, such as diarrhoea, flatulence, and adverse gastrointestinal symptoms (Sivasothy *et al.*, 2016; Sun *et al*., 2016). Hence, it is of interest to identify effective natural plant-derived α-glucosidase inhibitors devoid of side effects.

---

* Corresponding author (khalijah@um.edu.my; https://orcid.org/0000-0001-5971-6570)

Nauclea subdita (Korth.) Steud. and *Alpinia pahangensis* Ridley are two medicinal plants from Malaysia with the latter being endemic to the state of Pahang. *N. subdita* has traditionally been used to treat many ailments such as fever, pain, dental caries, oral septic, malaria, dysentery, diarrhoea, and central nervous system-related diseases (e.g epilepsy) (Aisiah *et al.*, 2019). *A. pahangensis* on the other hand has only been reported to have been used by the tribal natives of Pahang to relieve flatulence (Phang *et al.*, 2013). Previous study has reported that the ethanol extract of *Nauclea subdita* is able to decrease the blood glucose level of mice with 25.45% at the dosage of 250 mg/20 g body weight. (Diana, 2017). Besides, pahangensin A, a bis-labdanic diterpene isolated from *A. pahangensis* has shown to exhibit stronger inhibitory effects towards α-amylase and α-glucosidase in comparison to acarbose (Loo *et al.*, 2019).

Phytochemical investigation of the bark of *N. subdita* and the rhizomes of *A. pahangensis* by our group has yielded indole alkaloids and labdane diterpenes respectively as the major class of secondary metabolites in these medicinal plants (Sivasothy *et al.*, 2013a; 2013b; 2014; Liew *et al.*, 2014). In addition, a large number of plants and plant derived constituents, for example, terpenes, alkaloids, flavonoids, and phenols have been known to exhibit anti-diabetic activities (Sivasothy *et al*., 2016; Tran *et al.*, 2020) With regard to this, although *N. subdita* and *A. pahangensis* have never been reported to be traditionally used to treat diabetes, it would be worthwhile to investigate their potential as a source of α-glucosidase inhibitors since the bark of *N. subdita* and the rhizomes of *A. pahangensis* are rich in alkaloids and terpenoids, respectively. Hence, in the present paper, the α-glucosidase inhibitory activity of the major compounds, an indole alkaloid from *Nauclea subdita* (Korth.) Steud. and two labdane diterpenes from *Alpinia pahangensis* Ridley, along with their enzyme kinetic and molecular docking studies, are reported.

MATERIALS AND METHODS

General experimental procedures and plant materials

The general procedures were the same as those previously described (Liew *et al.*, 2014; Sivasothy *et al*., 2013b). *Nauclea subdita* (Korth.) Steud. (Rubiaceae), and *Alpinia pahangensis* Ridley. (Zingiberaceae) were collected from Perak and Pahang (Malaysia), respectively. Their voucher specimens KL 5254, and KU 001, respectively) were deposited in the Herbarium of the Department of Chemistry, Universiti Malaya, Kuala Lumpur, Malaysia.

Extraction, isolation, and characterization of compounds 1-3

Compounds **1-3** were extracted, purified, and characterized according to previously described methods (Sivasothy *et al*., 2013b; Liew *et al.*, 2014).

α-glucosidase inhibitory assay

The inhibition of the α-glucosidase enzyme (E.C.3.2.1.20 from *Saccharomyces cerevisiae*) was measured spectrophotometrically at 37 °C with the addition of 0.5 mM substrate (*p*-nitrophenyl α-D-glucopyranoside), 50 mM of phosphate saline buffer (pH 6.8) to a 96-well plate, followed by the addition of the test samples (20 μL/well), prepared in 70% DMSO. The reaction was initiated with the addition of the enzyme (0.2 units/mL), prepared in 50 mM sodium phosphate buffer containing 100 mM NaCl. Standard drug acarbose was used as the positive control. The absorbance at 400 nm, due to the hydrolysis of the substrate by α-glucosidase, was observed continuously with a multi-plate spectrophotometer (Spectra Max, Molecular Devices, U.S.A.). Measurements were carried out in triplicate for each experiment (Sivasothy *et al*., 2013b; Liew *et al*., 2014). The percentage of inhibition was calculated according to the following formula:

Inhibitory activity (%) = (OD Control – OD Test sample) / OD Control × 100

Enzyme kinetics

Enzyme kinetic studies were performed to evaluate the mechanism of inhibition and therapeutic potential of the active compounds. The inhibitory potential of the active compounds, as well as their inhibition types, were inferred from the Lineweaver-Burk plot, secondary replot of the Lineweaver-Burk plot, and the Dixon plot. The

Lineweaver-Burk plot is the plot of reciprocal of the rate of reaction against the reciprocal of the concentrations of substrate, while the secondary replot of the Lineweaver-Burk plot was used to study the inhibitory effect of the compounds on K_m and V_{max}. The K_i values were determined by plotting the slope of each line against different inhibitory concentrations. The reciprocal of the rate of reaction, plotted against various inhibitor concentrations, represented as the Dixon plot, and reconfirmed the K_i values. Kinetic parameters were calculated using the GraFit software, where [I] and [S] are the total concentrations of the inhibitor and substrate, respectively. K_m is the Michaelis constant, and $K_{m\ app}$ is the apparent Michaelis constant. V_{max} is the maximum reaction velocity, and $V_{max\ app}$ is the apparent maximum reaction velocity of the α-glucosidase enzyme with the substrate *p*-nitrophenyl α-D-glucopyranoside. K_i and K_i' are the inhibition constants of the inhibitors (Sivasothy *et al*., 2013b; Liew *et al*., 2014).

Molecular docking

α-Glucosidase from *Aspergillus awamori* has a 24% sequence similarity with its human counterpart. Interestingly relatively high sequence similarity of 34% to 59% in the *C*-terminal of the enzyme (*i.e.,* the catalytic domain). In humans and *Aspergillus awamori,* α-glucosidase enzymes show almost similar pH, substrate specificity and inhibitor sensitivity. In the enzyme of both the species, the modification in residues such as arginine, tryptophan or cysteine adversely affects the enzymatic activity. Hence, to identify the inhibitors against human α-glucosidase, *Aspergillus awamori* α-glucosidase is used as a model (Faridmoayer & Scaman, 2004).

Crystal structure of α-glucosidase with PDB ID 1AGM, 2.4 Å resolution was used as the target protein. The water and ligand molecules were removed from the original crystal structure and modified according to the CHARMm force field with partial charge Momany-Rone (Momany & Rone, 1992). Short minimizations of the structures were performed with a root mean square (RMS) gradient tolerance of 0.1000 kcal/(mol × Angstrom), satisfied in Discovery Studio 2.5 (Accelrys Discovery Studio, 2009). The ligands were obtained from PubChem compound (*http://www.ncbi.nlm.nih.gov/pccompound*), and optimized based on functional B3LYP, the basis set of 6-31G* (d,p) in Gaussian 09 before being minimized using the same protocol employed for the target protein. AUTODOCK VINA (Trott & Olson, 2010) program was used for rigid docking of the ligands into the binding site (ARG52, ASP53, LEU174, GLU176, ARG301, and GLU395) of the target protein.

Molecular dynamics (MD) simulations and binding free energy calculations

Since compounds **1** and **2** were found to be more active as compared to compound **3**, they were selected along with acarbose for MD simulation using PMEMD. CUDA (Götz *et al.*, 2012; Le Grand *et al.*, 2013; Salomon-Ferrer *et al.*, 2013) from AMBER 12 on GPUs Quadro 2000D produced by NVIDIA, which speeds up the simulation wall time required to obtain the trajectory files from each simulation. Prior to that the ligands were sent to the RESP ESP charge derive server to generate the general force field parameters (GAFF), and to build the force field library (Vanquelef *et al.*, 2011). The structures of the protein-ligand complex were solvated in a cubic box of TIP3P water (Jorgensen *et al.*, 1983), extending at least 10 Å in each direction from the solute and the force field 12 (ff12SB). To neutralize the counter ion, Na^+ ions were added to the protein-ligand complex, and the cut-off radius was kept to 20 Å to compute the non-bonded interactions. All simulations were performed under periodic boundary conditions (Weber *et al.*, 2000), and long-range electrostatic were treated based on the Particle-Mesh-Ewald (PME) methods (Darden *et al.*, 1993; Essmann *et al.*, 1995). The SHAKE algorithm and Langevin dynamics were applied to constrain the bonds that involved hydrogen, and to control the temperature (Weber *et al.*, 2000). The temperature of each system was gradually increased from 0 to 310.15 K, over a period of 60 ps of NVT dynamics. Later on, 300 ps of NPT equilibration at 310.15 K, and 1 atmosphere pressure, followed by 10,000 ps of NPT-MD simulation were carried out. The trajectories were analysed using the PTRAJ module of the amber package.

The binding free energy of each complex was estimated, based on the MM-PBSA (Molecular Mechanics Poisson-Boltzmann Surface Area; Kollman *et al.*, 2000), and MM-GBSA (Molecular Mechanics Generalized Born Solvent Area; Chong *et al.*, 1999) protocols from 6–10 ns of the trajectories. A total of 500 snapshots were collected from each range, and the complex interaction energy profiles were generated by decomposing the total

binding free energies into residue-residue interaction pairs by the MM-GBSA decomposition process in the *mm_pbsa* program of AMBER 12.

RESULTS AND DISCUSSION

α-Glucosidase inhibitory assay

Angustine (**1**), (*E*)-labda-8(17),12-dien-15,16-dial (**2**), and zerumin A (**3**) (Figure 1) were evaluated for *in vitro* α-glucosidase inhibitory activity. Compounds **1** (IC_{50} = 48.1 ± 2.5 μM), **2** (IC_{50} = 39.7 ± 1.09 μM), and **3** (IC_{50} = 53.3 ± 2.94 μM) demonstrated significantly high inhibitory activity as compared to the standard inhibitor drug, acarbose (IC_{50} = 840 ± 1.73 μM). Results are summarized in Table 1, and Figure 2.
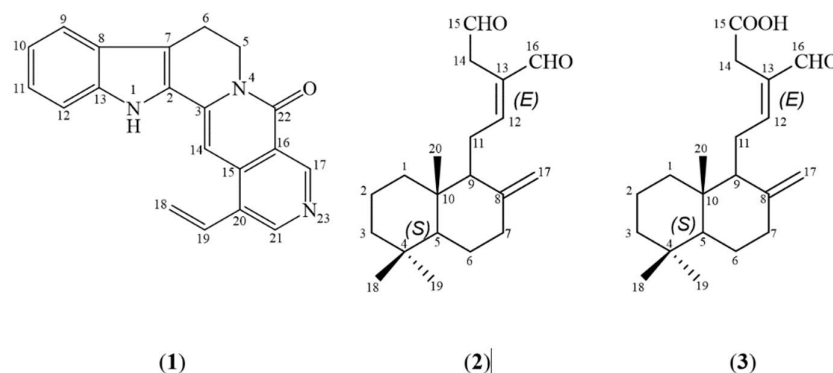
Figure 1: The structures of angustine (**1**), (*E*)-labda-8(17),12-dien-15,16-dial (**2**), and zerumin A (**3**)
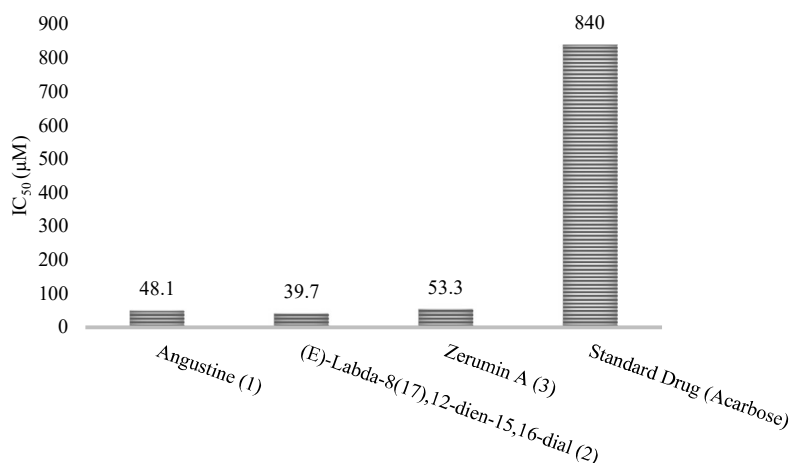
Figure 2: Inhibition of α-glucosidase by angustine (**1**), (*E*)-labda-8(17),12-dien-15,16-dial (**2**), and zerumin A (**3**)

Table 1: Results of molecular docking of α-glucosidase with compounds **1-3** AutodockVina

| Receptor	Ligands	IC_{50} ± SEM (*μM*)	Binding affinity (kcal/mol)
	Angustine (**1**)	48.1 ± 2.5	-9.5-(-6.5)
α-Glucosidase	(*E*)-Labda-8(17),12-dien-15,16-dial (**2**)	39.7 ± 1.09	-7.2-(-6.0)
	Zerumin A (**3**)	53.3 ± 2.94	-7.8-(-6.6)
	Standard (Acarbose)	840 ± 1.73	-9.8-(-9.1)

IC_{50} Values expressed as SEM (standard error of mean), where n=3

Enzyme kinetics

The mechanism of inhibition of the most potent compounds and their interactions with the amino acid residues were evaluated. Compounds **1**, **2**, and **3** with Ki values 46, 55, and 34 μM, respectively, inhibited the α-glucosidase enzyme in a concentration dependent manner. Kinetic studies of compound **1** revealed a mixed-type inhibition, whereas compound **2** was found to inhibit α-glucosidase in a non-competitive type manner with no change in enzyme Km, which showed that the binding of the enzyme to the substrate was not affected by the inhibitor, and it only reduced the enzyme concentration. Compound **3** was also identified as a non-competitive inhibitor. The standard α-glucosidase inhibitor drug (Acarbose) with a Ki value of 700 μM showed a competitive mode of inhibition, indicating that acarbose interacts with the amino acid residues of the active site of the enzyme (Table 2, Figures 3-5).

Table 2: Kinetic parameters of inhibition of α-glucosidase enzyme by compounds **1-3**

| Compounds	V_{max} (μmol/min^{-1})	V_{maxapp} (μmol/min^{-1})	K_m (mM)	K_{mapp} (mM)	K_i (μM)	Type of inhibition
Angustine (**1**)	43	44	1.74	1.13	46	Mixed-type
(*E*)-Labda-8(17),12-dien-15,16-dial (**2**)	58.4	1.54	1.29	0.73	55	Non-Competitive
Zerumin A (**3**)	72.9	34	2.23	2.34	34	Non-Competitive
Standard (Acarbose)	43	41	0.8	1.38	700	Competitive
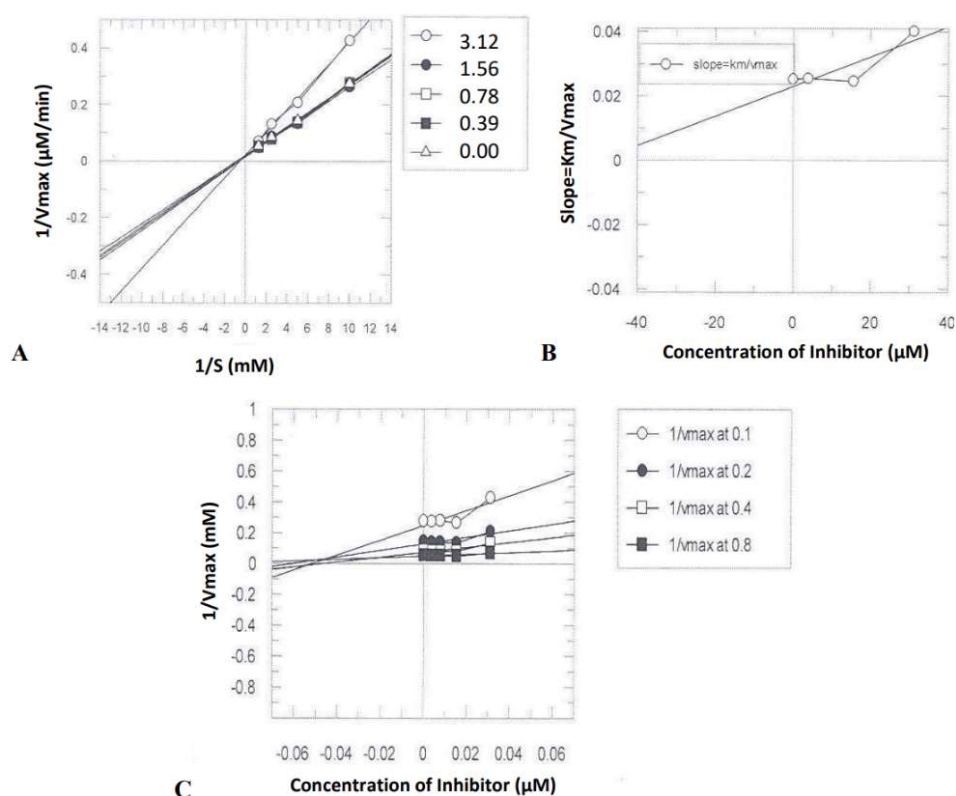
Figure 3: Inhibition of α-glucosidase by angustine (**1**).
A. Lineweaver-Burk plot (reciprocal of rate of reaction *versus* reciprocal of substrate in the absence, and presence of 12.5, 6.25, 3.12, 1.56, 0.78, and 0.39 μM of compound **1**); B. Secondary replot of Lineweaver-Burk plot (slopes of each line *versus* different concentrations of compound **1**); C. Dixon plot (reciprocal of rate of reaction *versus* different concentrations of compound **1**)

Binding affinity with protein targets from the *in silico* molecular docking study

Docking studies were performed to gain insight into the preferable binding conformation of the ligands with the target protein. The results with the rigid docking indicated that the ligands were active with negative binding affinity range (kcal/mol) of possible binding poses of -9.5 – (-6.5), -7.2 – (-6.0), -7.8 – (-6.6), and -9.8 – (-9.1) kcal/mol, respectively, as shown in Table 1. The lower the value of the binding affinity, the stronger is the interaction between the receptor and peptides, therefore indicating that the peptides are in their most stable conformation (Spratt & Greenwood, 2000). The MD simulation complexes of 10 ns trajectory were visualized using discovery studio, as depicted in Figure 6. In the representation, ligands A) Angustine, B) (*E*)-labda-8(17), 12-dien-15,16-dial, and C) acarbose which have been illustrated in blue, red, and yellow respectively, were observed with important amino acid residue(s) that contributed negative value(s) in the 3 Å region. A close view of the interactions has shown that the green dotted lines represent the hydrogen bonds. Several hydrogen bonds were observed between acarbose at A:ARG52:HH12 - ACR:O1D, A:ARG52:HH12 - ACR:O2D, A:ARG52:HH22 - ACR:O2D, ACR:H43 - A:GLU176:OE1, ACR:H45 - A:GLU177:OE2, ACR:H39 - A:GLU176:OE1, and ACR:H41 - A:GLU176:OE1. Only one hydrogen bond was observed for (*E*)-labda-8(17), 12-dien-15,16-dial (**2**) at A:SER406:H-(E)-labda:O16, whereas none was found in Angustine (**1**).
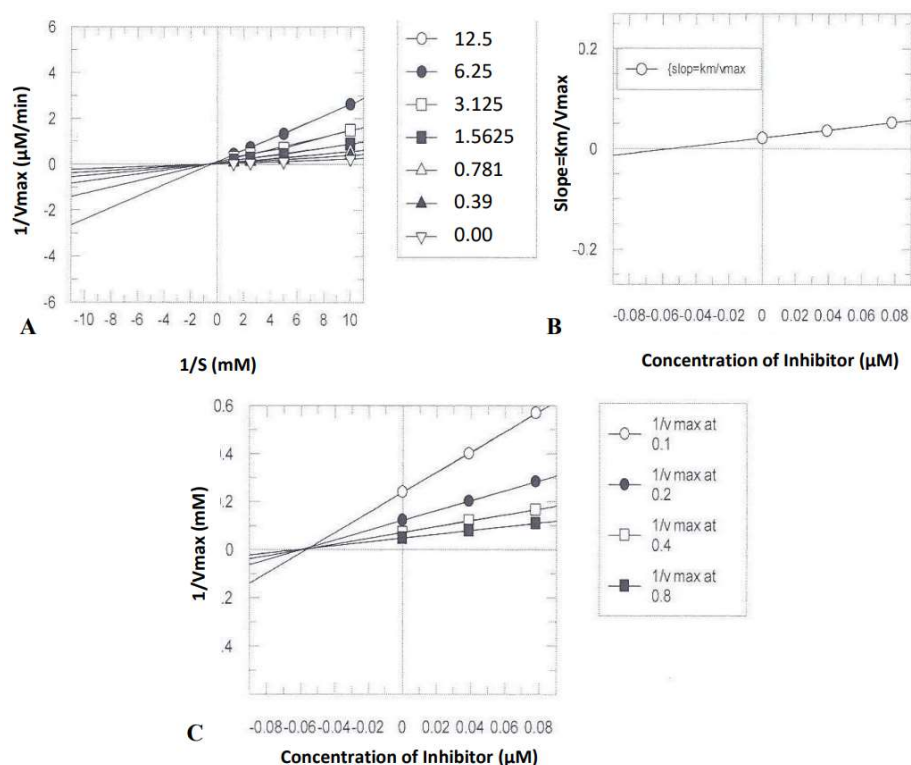

Figure 4: Inhibition of α-glucosidase by (E)-labda-8(17),12-dien-15,16-dial (**2**).
A. Lineweaver-Burk plot (reciprocal of rate of reaction *versus* reciprocal of substrate both in the absence, and presence of 12.5, 6.25, 3.12, 1.56, 0.78, and 0.39 *µ*M of compound **2**); B. Secondary replot of Lineweaver-Burk plot (slopes of each line *versus* different concentrations of compound **2**); C. Dixon plot (reciprocal of rate of reaction *versus* different concentrations of compound **2**)
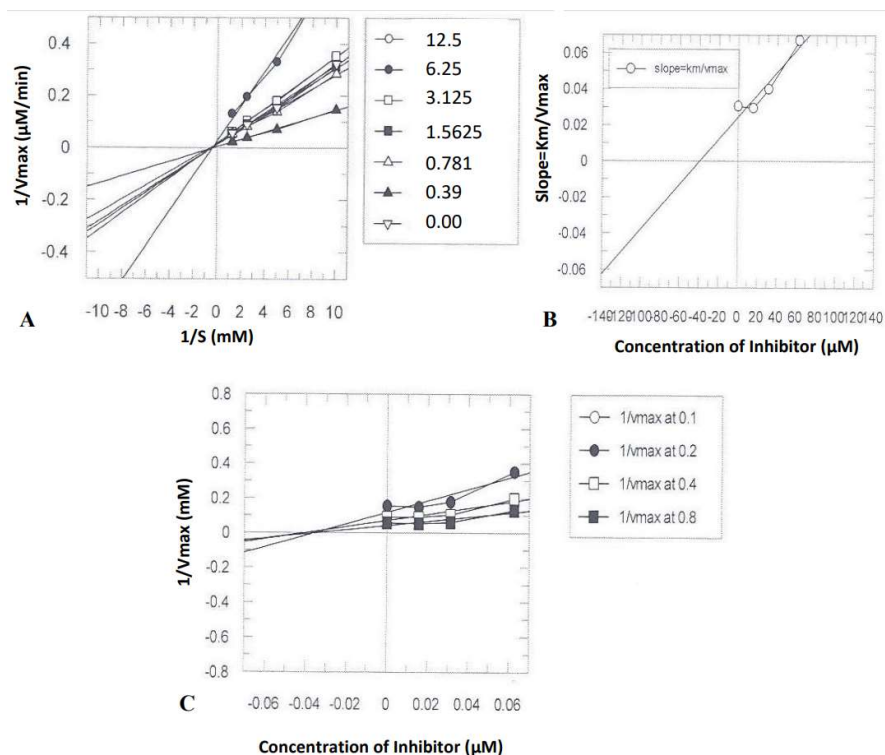
**Figure 5:** Inhibition of α-glucosidase by zerumin A (**3**)
A. Lineweaver-Burk plot (reciprocal of rate of reaction *versus* reciprocal of substrate both in the absence, and presence of 12.5, 6.25, 3.12, 1.56, 0.78, and 0.39 *μ*M of compound **3**); B. Secondary replot of Lineweaver-Burk plot (slopes of each line *versus* different concentrations of compound **3**); C. Dixon plot (reciprocal of rate of reaction *versus* different concentrations of compound **3**)
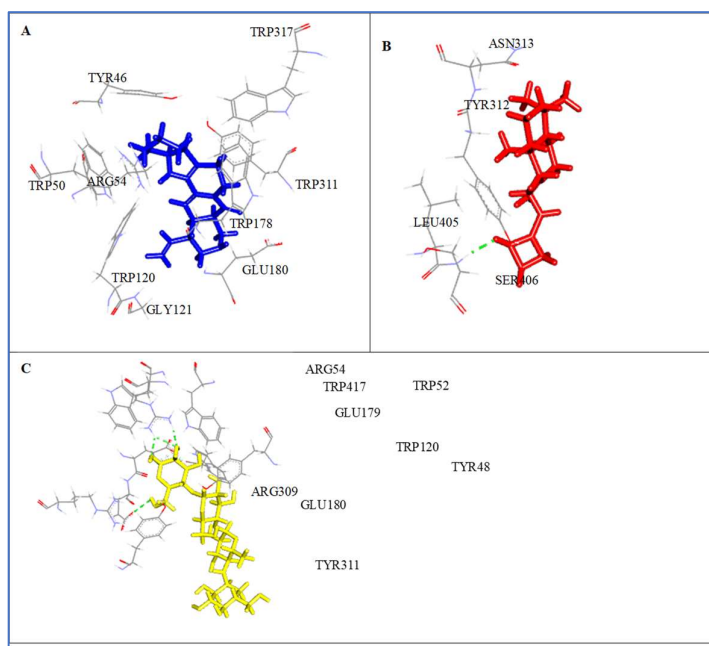
Figure 6: Interaction between α-glucosidase and the ligands with 3 Å region with hydrogen bonds. **A** angustine (**1**) (blue), **B** (*E*)-labda-8(17),12-dien-15,16-dial (**2**) (red), and **C** acarbose (yellow) at 10 ns simulation time.

Dynamics conformational changes of the protein-ligand complex

The trajectory stability was monitored, and confirmed by the analysis of the root mean squared deviations (RMSD) of all of the Cα-atoms in Figure 7. Based on the docking results, the top-ranked conformations of ligands were selected for further studies in the MD simulation(s). The RMSD values fluctuated upon reaching a maximum of about 2.52 Å, 2.50 Å, and 2.77 Å for angustine (**1**), (*E*)-labda-8(17),12-dien-15,16-dial (**2**), and acarbose at 6 ns, 9 ns and 6 ns, respectively. During the simulation time, angustine (**1**) was observed to oscillate steadily within a small range as compared to the other two ligands.
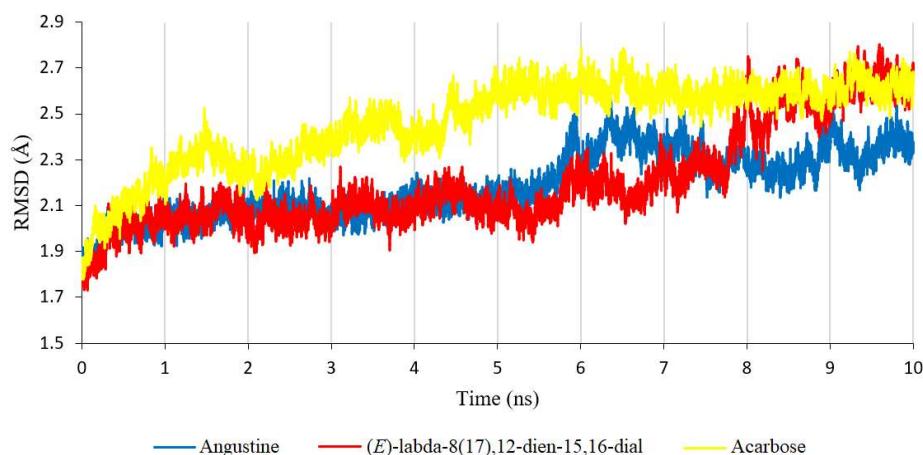
Figure 7: Root mean squared deviations (RMSD) of all C$_\alpha$-atoms of α-glucosidase with angustine (**1**) (blue), (*E*)-labda-8(17),12-dien-15,16-dial (**2**) (red), and acarbose (yellow) against simulation

Table 3: MM-PBSA/GBSA calculation during 6–10 ns of the MD simulations for α-glucosidase and selected ligands **1** and **2**

Method	Contribution	Energy in each contribution (kcal/mol) from 6–10 ns		
		Angustine (**1**)	(*E*)-Labda-8(17),12-dien-15,16-dial (**2**)	Standard (Acarbose)
MM	ELE	-5.60 ± 1.65	-3.21 ± 2.11	-66.51 ± 9.59
	VDW	-38.59 ± 2.04	-21.62 ± 1.93	-24.80 ± 4.04
	GAS	-44.19 ± 2.52	-24.83 ± 2.97	-91.32 ± 8.32
PBSA	PB$_{SUR}$	-4.93 ± 0.15	-4.21 ± 0.19	-5.01 ± 0.37
	PB$_{CAL}$	33.43 ± 3.41	21.30 ± 3.68	86.15 ± 8.69
	PB$_{SOL}$	28.50 ± 3.35	17.09 ± 3.57	81.15 ± 8.61
	PB$_{ELE}$	27.83 ± 3.26	18.09 ± 3.43	19.64 ± 8.90
	PB$_{TOT}$	-15.69 ± 3.35	-7.74 ± 3.05	-10.17 ± 6.70
GBSA	GB$_{SUR}$	-2.79 ± 0.10	-1.90 ± 0.16	-3.10 ± 0.24
	GB$_{CAL}$	23.40 ± 1.61	14.04 ± 1.93	88.19 ± 7.16
	GB$_{SOL}$	20.61 ± 1.59	12.13 ± 1.85	85.09 ± 7.13
	GB$_{ELE}$	17.79 ± 1.11	10.83 ± 1.46	21.68 ± 4.84
	GB$_{TOT}$	-23.58 ± 2.13	-12.70 ± 1.77	-6.23 ± 3.47

Note: ELE accounts for the electrostatic interaction, VDW denotes the Van der Waals interactions, GAS accounts for the addition ELE+ VDW + INT being the binding enthalpic contributions in vacuo, PB$_{SUR}$ accounts for the non-polar contribution to solvation, PB$_{CAL}$ is the polar contribution of salvation, PB$_{SOL}$ for the PB$_{SUR}$ + PB$_{CAL}$, PB$_{ELE}$ denotes the PB$_{CAL}$ + ELE addition, and PB$_{TOT}$ accounts for the total binding free energy calculated by the MM-PBSA method.
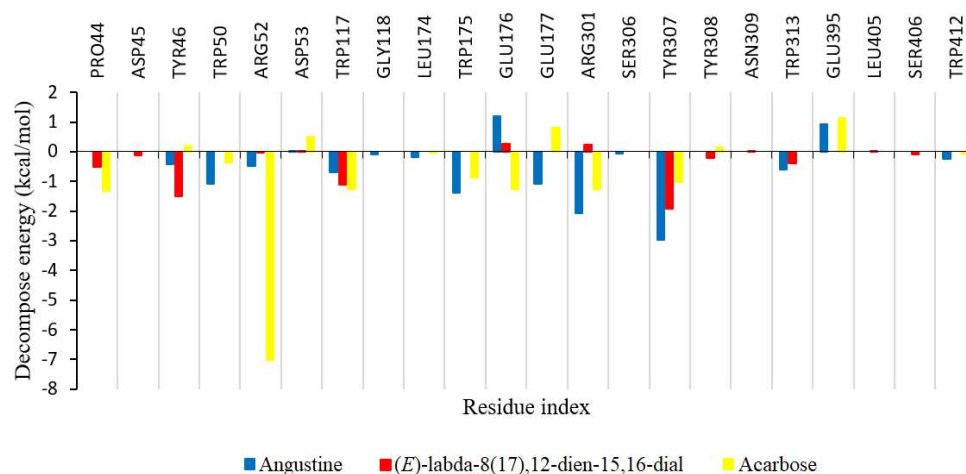
Binding free energy of the complex

The contribution of energies and the binding free energy of each complex are tabulated in Table 3. The calculations from MM-GBSA between 6 and10 ns were approximate to the experimental value with a lower standard error of the mean, whereas the MM-PBSA protocol did not give any good correlation. Angustine (**1**) showed a lower GB_{TOT} value of -23.58 kcal/mol, as compared to (*E*)-labda-8(17),12-dien-15,16-dial (-12.70 kcal/mol) (**2**), and acarbose (-6.23 kcal/mol) during 6-10 ns of simulation with α-glucosidase. The main contribution of energy was from the Van der Waal's forces, rather than the electrostatic forces, for both angustine (**1**), and (*E*)-labda-8(17),12-dien-15,16-dial (**2**), while it was *vice versa* for the binding of acarbose. For a protein-ligand complex, properties which are calculated based on the MM-GBSA protocol are more often reported in the literature as they provide better correlations with the experimental results.

Important amino acid residues involved in binding of the complex

Binding free energies of each complex were analysed to investigate the important amino acid residues that showed strong interactions with the target proteins. Figure 8 illustrates the results of this analysis by plotting the decomposed energies against significant amino acids residues of each complex. The positive and negative values indicate the unfavourable and favourable contributions respectively. Residues which contribute to a large relative energy (< -1 kcal/mol) were considered as the key amino acid residues of the complex, while residues TRP50, TRP175, GLU 177, ARG301, and TYR307 were identified to have a significant contribution to the binding energy of angustine (**1**) with negative energy values of -1.08, -1.37 -1.07, -2.06, and -2.98 kcal/mol, respectively. TYR46, TRP117, and TYR307 were identified as important amino acids residues for (*E*)-labda-8(17),12-dien-15,16-dial (**2**) with the energy contributions of -1.5, -1.1, and -1.91 kcal/mol, respectively. Acarbose forms contact with important amino acids of PRO44, ARG52, TRP117, GLU176, ARG301, and TYR307 with energy values of -1.32, -7.03 -1.26, -1.25, -1.27 and-1.03 kcal/mol, respectively.

Figure 8: Decomposition of binding free energy on a per residue within 3 Å, including binding site region of α-glucosidase during 6-10 ns simulations

Since angustine (**1**) and (*E*)-labda-8(17),12-dien-15,16-dial (**2**) have better binding activities as compared to acarbose, the best conformations of angustine (**1**), and (*E*)-labda-8(17),12-dien-15,16-dial (**2**) were generated from their respective docking experiments and selected to perform the MD simulation to study their binding mechanisms and compared with acarbose. MD simulation was not performed for zerumin A (**3**), as it exhibited a lower activity as compared to other the two ligands. The RMSD values showed angustine (**1**) to be better in stability over simulation time. The MM-GBSA calculations revealed that angustine (**1**) had the lowest energy value as compared to the other two ligands, thus indicating it to be the most stable with the most favourable binding. Therefore, the kinetic study for angustine (**1**) showed a good correlation with the experimental results,

and thus it was identified as a potent α-glucosidase inhibitor. The analyses of the decomposed energy during 6–10 ns were carried out, however, for long-term MDs simulations at least 100 ns will be needed to explore in more detail to gain accurate details for the new drug discovery, design, and development. From our observation, ARG52 and ARG301 were identified as the key residues which bind with angustine (**1**) and acarbose, as they contributed to the negative value of the decomposed energy and were present at the binding site, which similarly found in the Xray complexes. ARG52 has a negative energy of -7.03 kcal/mol since it is able to form three hydrogen bonds with acarbose as compared to -0.47 kcal/mol for angustine (**1**). This indicated that ARG52 may have played a crucial role in binding with the ligands acarbose, and angustine (**1**). SER406 showed an energy value of -0.1 kcal/mol with (*E*)-labda-8(17),12-dien-15,16-dial (**2**), whereby this amino acid was apparently involved in the formation of the hydrogen bond.

CONCLUSION

This study involved the biochemical assay and study of kinetic patterns, molecular docking, the inhibitory aspects and binding modes of three natural compounds as α-glucosidase inhibitors. Through this study, potent natural α-glucosidase inhibitors were identified. Kinetic studies indicated that the compounds with electron donating groups take part in binding with the amino acid residues of the enzyme, α-glucosidase. This idea can be used for rational drug design toward the development of more effective inhibitors for therapeutic purposes. These lead molecules need to be further investigated *in-vivo* as anti-diabetic agents. From the knowledge of the binding conformation between the ligands and the target protein resulting from the molecular docking and MD simulation, angustine (**1**) was identified as a potential lead α-glucosidase inhibitor.

Acknowledgement

Conflicts of Interest

The authors declare no conflict of interest.

REFERENCES

Accelrys Discovery Studio (2009). Discovery Studio (Version Version 2.5.5). Accelrys Inc., San Diego, CA, USA.

Aisiah S., Prajitno A., Maftuch M. & Yuniarti A. (2019). The potential of bangkal leaf (N*auclea subdita* [Korth.] Steud.) extract as antibacterial in catfish *Pangasius hypophthalmus* culture **12**(6): 2093–2102.

Chong L.T., Duan Y., Wang L., Massova I. & Kollman P.A. (1999). Molecular dynamics and free-energy calculations applied to affinity maturation in antibody 48G7. *Proceedings of the National Academy of Sciences of the United States of America* **96**(25): 14330–14335.

Darden T., York D. & Pedersen L. (1993). Particle mesh Ewald: An N log(N) method for Ewald sums in large systems. *The Journal of Chemical Physics* **98**(12): 10089–10092.
  DOI: http://dx.doi.org/10.1063/1.464397

Diana L.R. (2017). Uji aktivitas antidiabetes ekstrak etanol 70% daun taya (*Nauclea Subdita* (Korth) Steud) terhadap mencit putih (*Mus Musculus* L.) dengan induksi aloksan. *Indonesia Natural Research Pharmaceutical Journal* **2**(2): 79–87.

Essmann U., Perera L., Berkowitz M.L., Darden T., Lee H. & Pedersen L.G. (1995). A smooth particle mesh Ewald potential. *The Journal of Chemical Physics* **103**(19): 8577–8593.

Faridmoayer A. & Scaman C.H. (2004). An improved purification procedure for soluble processing alpha-glucosidase I from *Saccharomyces cerevisiae* overexpressing CWH41. *Protein Expression and Purification* **33**(1): 11–18.
  DOI: http://dx.doi.org/10.1016/j.pep.2003.09.013

Götz A.W., Williamson M.J., Xu D., Poole D., Le Grand S. & Walker R.C. (2012). Routine microsecond molecular dynamics simulations with AMBER on GPUs. 1. Generalized born. *Journal of Chemical Theory and Computation* **8**(5): 1542–1555.
  DOI: http://dx.doi.org/10.1021/ct200909j

Jorgensen W.L., Chandrasekhar J., Madura J.D., Impey R.W. & Klein M.L. (1983). Comparison of simple potential functions for simulating liquid water. *The Journal of Chemical Physics* **79**(2): 926–935.
  DOI: http://dx.doi.org/10.1063/1.445869

Kollman P.A. *et al.* (15 authors) (2000). Calculating structures and free energies of complex molecules: combining molecular mechanics and continuum models. *Accounts of Chemical Research* **33**(12): 889–897.

DOI: http://dx.doi.org/10.1021/ar000033j

Le Grand S., Götz A.W. & Walker R.C. (2013). SPFP: Speed without compromise—A mixed precision model for GPU accelerated molecular dynamics simulations. *Computer Physics Communications* **184**(2): 374–380.
DOI: http://dx.doi.org/10.1016/j.cpc.2012.09.022

Liew S.Y., Looi C.Y., Paydar M., Cheah F.K., Leong K.H., Wong W.F., Mustafa M.R., Litaudon M. & Awang K. (2014). Subditine, a new monoterpenoid indole alkaloid from bark of *Nauclea subdita* (Korth.) Steud. induces apoptosis in human prostate cancer Cells. *PLoS ONE* **9**(2): e87286.
DOI: http://dx.doi.org/10.1371/journal.pone.0087286

Liu D. *et al.* (13 authors) (2016). Design, synthesis and biological evaluation of 3′-benzylated analogs of 3′-*epi*-neoponkoranol as potent α-glucosidase inhibitors. *European Journal of Medicinal Chemistry* **110**: 224–236.
DOI: http://dx.doi.org/10.1016/j.ejmech.2016.01.029

Loo K.Y., Leong K.H., Sivasothy Y., Ibrahim H. & Awang K. (2019). Molecular insight and mode of inhibition of α-glucosidase and α-amylase by pahangensin a from *Alpinia pahangensis* Ridl. *Chemistry and Biodiversity* **16**(6): e1900032.
DOI: http://dx.doi.org/10.1002/cbdv.201900032

Momany F.A. & Rone R. (1992). Validation of the general purpose QUANTA ®3.2/CHARMm® force field. *Journal of Computational Chemistry* **13**(7): 888–900.
DOI: http://dx.doi.org/10.1002/jcc.540130714

Phang C.W., Malek S.N. & Ibrahim H. (2013). Antioxidant potential, cytotoxic activity and total phenolic content of Alpinia pahangensis rhizomes. *BMC Complementary and Alternative Medicine* **13**: 243.
DOI: http://dx.doi.org/10.1186/1472-6882-13-243

Salomon-Ferrer R., Götz A.W., Poole D., Le Grand S. & Walker R.C. (2013). Routine microsecond molecular dynamics simulations with AMBER on GPUs. 2. explicit solvent particle mesh Ewald. *Journal of Chemical Theory and Computation* **9**(9): 3878–3888.
DOI: http://dx.doi.org/10.1021/ct400314y

Simpson B.K., Nollet L.M.L., Toldrá F., Benjakul S., Paliyath G. & Hui Y.H. (2012). *Food Biochemistry and Food Processing*, 2nd edition. John Wiley & Sons, New York, USA.

Sivasothy Y., Ibrahim H., Paliany A.S., Alias S.A. & Awang K. (2013a). Pahangensin A and B, two new antibacterial diterpenes from the rhizomes of *Alpinia pahangensis* Ridley. *Bioorganic and Medicinal Chemistry Letters* **23**(23): 6280–6285.
DOI: https://doi.org/10.1016/j.bmcl.2013.09.082

Sivasothy Y., Ibrahim H., Paliany A.S., Alias S.A., Md Nor N.R. & Awang K. (2013b). A new bis-labdanic diterpene from the rhizomes of *Alpinia pahangensis*. *Planta Medica* **79**(18): 1775–1780.
DOI: http://dx.doi.org/10.1055/s-0033-1351075

Sivasothy Y., Loo K.Y., Leong K.H., Litaudon M. & Awang K. (2016). A potent alpha-glucosidase inhibitor from *Myristica cinnamomea* King. *Phytochemistry* **122**: 265–269.
DOI: http://dx.doi.org/10.1016/j.phytochem.2015.12.007

Sivasothy Y., Zachariah C.C.K., Leong K.H., John S.K.S., Ibrahim H. & Awang K. (2014). A novel heptacyclic diterpene from Alpinia pahangensis Ridley, a wild ginger endemic to Malaysia. *Tetrahedron Letters* **55**(45): 6163–6166.
DOI: https://doi.org/10.1016/j.tetlet.2014.08.115

Spratt B.G. & Greenwood B.M. (2000). Prevention of pneumococcal disease by vaccination: does serotype replacement matter? *The Lancet* **356**(9237): 1210–1211.
DOI: http://dx.doi.org/10.1016/S0140-6736(00)02779-3

Sun S., Kadouh H.C., Zhu W. & Zhou K. (2016). Bioactivity-guided isolation and purification of α-glucosidase inhibitor, 6-*O-D*-glycosides, from Tinta Cão grape pomace. *Journal of Functional Foods* **23**: 573–579.
DOI: http://dx.doi.org/10.1016/j.jff.2016.03.009

Tran N., Pham B. & Le L. (2020). Bioactive compounds in anti-diabetic plants: from herbal medicine to modern drug discovery. *Biology* **9**(9): 252.
DOI: http://dx.doi.org/10.3390/biology9090252

Trott O. & Olson A.J. (2010). AutoDock Vina: improving the speed and accuracy of docking with a new scoring function, efficient optimization and multithreading. *Journal of Computational Chemistry* **31**(2): 455–461.
DOI: http://dx.doi.org/10.1002/jcc.21334

Vanquelef E., Simon S., Marquant G., Garcia E., Klimerak G., Delepine, J.C., Cieplak P. & Dupradeau F.Y. (2011). R.E.D. Server: a web service for deriving RESP and ESP charges and building force field libraries for new molecules and molecular fragments. *Nucleic Acids Research* **39**(Issue Suppl. 2): W511–W517.

Weber W., Hünenberger P.H. & McCammon J.A. (2000). Molecular dynamics simulations of a polyalanine octapeptide under Ewald boundary conditions: influence of artificial periodicity on peptide conformation. *The Journal of Physical Chemistry B* **104**(15): 3668–3675.
DOI: http://dx.doi.org/10.1021/jp9937757

WHO (2016) *Global Report on Diabetes*. World Health Organization, Geneva, Switzerland.